Werk

Jahr: 1976
Kollektion: fid.geo
Signatur: 8 Z NAT 2148:42
Digitalisiert: Niedersächsische Staats- und Universitätsbibliothek Göttingen
Werk Id: PPN1015067948_0042
PURL: http://resolver.sub.uni-goettingen.de/purl?PPN1015067948_0042

LOG Id: LOG_0118
LOG Titel: Micrometeoroid orbits observable by the Helios micrometeoroid detector (E 10)
LOG Typ: article

Übergeordnetes Werk

Werk Id: PPN1015067948
PURL: http://resolver.sub.uni-goettingen.de/purl?PPN1015067948
OPAC: http://opac.sub.uni-goettingen.de/DB=1/PPN?PPN=1015067948

Contact

Niedersächsische Staats- und Universitätsbibliothek Göttingen
Georg-August-Universität Göttingen
Platz der Göttinger Sieben 1
37073 Göttingen
Germany
Email: gdz@sub.uni-goettingen.de

J. Geophys. 42, 737–741, 1977

Journal of Geophysics

Micrometeoroid Orbits Observable by the Helios Micrometeoroid Detector (E 10)

K.D. Schmidt

Bereich Extraterrestrische Physik, Ruhr-Universität Bochum,
Universitätsstraße 150, D-4630 Bochum, Federal Republic of Germany

Abstract. Sensor characteristics of the micrometeoroid detector (experiment 10) and Helios' spin and eccentric orbital motion give rise to selection effects. In this paper we discuss the influence of the spacecraft's motion on the computed osculating orbital elements (semimajor axis, eccentricity) of detectable dust particles. This constitutes a first step in the statistical treatment of dust orbits measured by Helios.

Key words: Interplanetary dust – Dust orbits.

The micrometeoroid detectors on board Helios detect dust particles in the interplanetary space along the spacecraft's orbit around the sun (Grün et al., 1976; Grün et al., 1977). The detectors are able to measure mass, speed, direction, chemical composition and charge of these particles. Therefore, in addition to information about spatial distribution, it is possible to compute orbital elements (here: semimajor axis and eccentricity) of the dust particles. But this it true only in a certain impact-velocity-range, where mass- and velocity-information can be separated. For this separation the upper impact velocity value is about $100\,\mathrm{km}\cdot\mathrm{s}^{-1}$, and it decreases when the mass of the impacting particle increases (Dietzel et al., 1973). For velocities exceeding $100\,\mathrm{km\,s}^{-1}$ only direction and composition are measurable. Both the mass- and velocity-information are necessary for orbit calculations. The orbital parameters may be calculated from the heliocentric location of the impact and from magnitude and direction of the velocity. These parameters change when the particle interacts with the solar electromagnetic radiation (radiation pressure, Poynting-Robertson-effect). The magnitude of these interactions depends, amongst other things (refractive index etc.) on the particle's radius (Schwehm, 1976) which may be roughly calculated by the measured mass and an assumed density.

The sum of the measured impact velocity ($\mathbf{v}_{\mathrm{imp}}$) and Helios' orbital velocity ($\mathbf{v}_{\mathrm{Hel}}$) yields the heliocentric dust velocity ($\mathbf{v}_d$) (see Fig. 1). Velocities due to the space probe's spin can be neglected here because they are about 3 orders of magnitude below the other velocities.

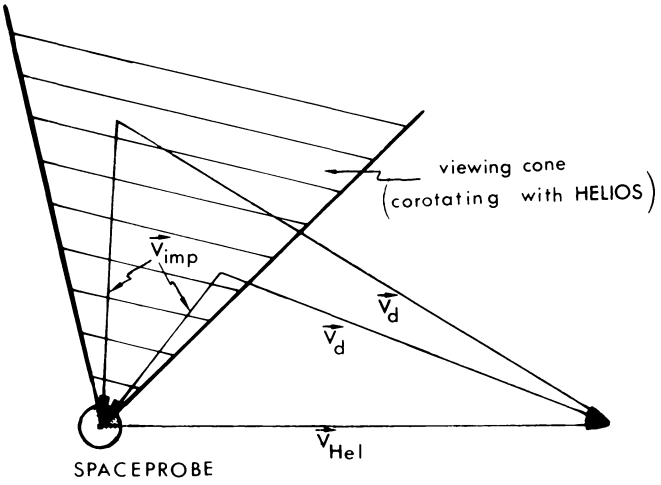

Fig. 1. Two examples of observable dust velocities (situation at impact)

All the dust velocities that can be observed during one spin period at one point on Helios' orbit and for which v_{imp} is less than or equal to $100\,km \cdot s^{-1}$ are transformed into osculating orbital elements, here: semimajor axis a and eccentricity e. This is done by means of the energy integral and Kepler's second law. The combinations of semimajor axis and eccentricity corresponding to the observable dust velocities make up areas in the $(1/a, e)$-plane, where by definition the semimajor axis of hyperbolic orbits ($e>1$) is counted negative. Elliptical orbits occur for $0<e<1$, whereas $e=0$ gives circular and $e=1$ parabolic and degenerated orbits.

$\mathbf{v}_d$ perpendicular to the Sun-Helios line yields the smallest eccentricity values for $e<1$, whereas the opposite is true for eccentricities greater than one. $\mathbf{v}_d$ parallel to this line results in degenerated orbits.

Figure 2 shows regions in the $(1/a, e)$-plane which are observable by the detector at different heliocentric distances r. These are calculated for $|v_{imp}| \leqq 100\,km \cdot s^{-1}$, and one example for another impact velocity limit is given.

The shape and size of these regions are affected by various parameters such as inclination i and radiation pressure β. For simplicity the following calculations are done in the ecliptic plane, but calculations of inclined orbits (dashed line in Fig. 2) or for the north or south viewing sensor respectively are similar.

For impact velocities up to $100\,km \cdot s^{-1}$ and for $\beta=0$ the regions in Figure 2 are surrounded by solid lines. These regions are the greatest ones, because in the ecliptic plane and for $|v_{imp}|=100\,km \cdot s^{-1}$ the highest dust velocities are measurable. The dotted line shows the decrease in the size of the regions, when for the upper impact velocity limit $50\,km \cdot s^{-1}$ ($r=0.6473$ AU) is assumed.

Figure 3 gives an idea of radiation pressure effects. Here the parameter is β, which is the ratio of radiation pressure and gravitational force acting on a dust particle. The increase of the regions with increasing β is evident.

Due to the upper impact velocity limit and due to the spin and orbital motion of Helios, not all dust velocities can be observed. Examples are given in

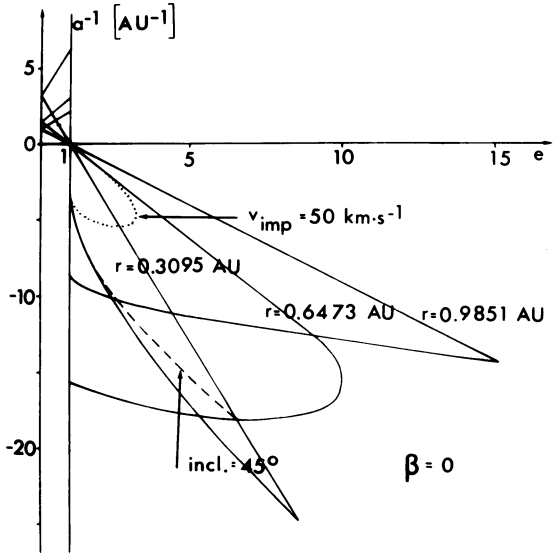

Fig. 2. Different observable regions in the $1/a$, e-plane

Figure 4, where relative observing times are given for different velocities at various distances from the sun. Here a viewing cone of 60° was assumed. Therefore a weighting of all the points in the $\frac{1}{a}-e$-plane has to be carried out, so that these points are weighted with respect to their observing times. The different observing times of dust velocities now correspond to a weighting along the $1/a$-axis, whereas selections of the angle between the sun-Helios line and the dust velocity transform into a weighting along the e-axis. The weighting over all the regions in the $(1/a, e)$-plane is achieved by taking into account the time Helios spends in the different distance intervals from the sun.

The above mentioned effects are global ones, whereas local effects, that is the angular sensibility of the sensors, play a role when starting backward calculations of dust orbits from measured impacts with a given position and a given viewing direction.

As pointed out earlier, heavier particles are detectable only at lower impact velocities. For example, the mass of an incoming particle has to be greater than $3 \cdot 10^{-13}$ g for velocities less than $10\,\mathrm{km \cdot s^{-1}}$. In this group we expect particles on bounded orbits spiralling towards the sun due to the Poynting-Robertson-effect. These particles will have orbital elements in the region for $e<1$ of the $(1/a, e)$-plane. For smaller particles mainly undergoing radiation pressure (β-meteoroids) we expect higher velocities, because they are on hyperbolic or highly eccentric orbits. Therefore, as far as we know, relevant regions in the $\frac{1}{a}-e$-plane are covered by the micrometeoroid sensors on board the two Helios-probes.

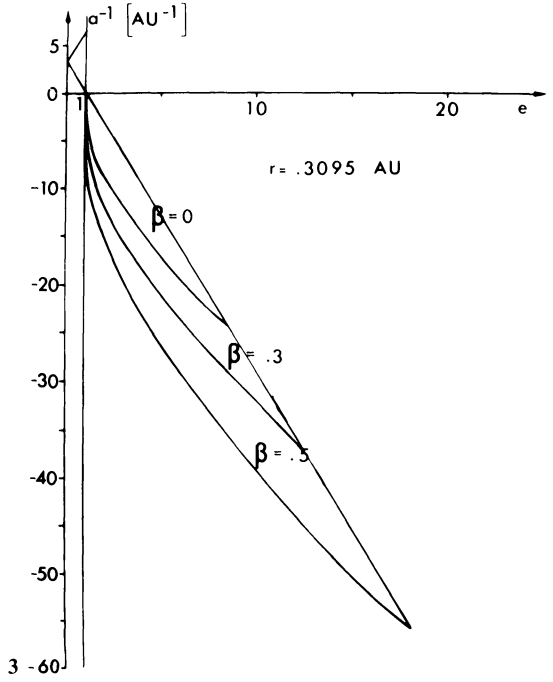

Fig. 3. Change of $1/a$, e-regions due to radiation pressure β

Fig. 4. Relative observing times of dust velocities at different heliocentric distances r (viewing cone of 60°)

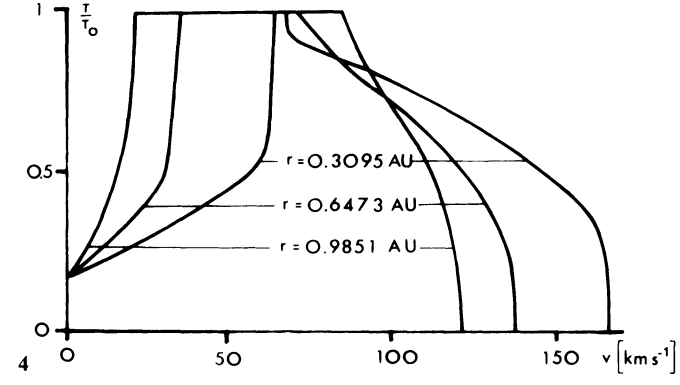

All the above mentioned statistics are the first step when starting a dynamic model of the interplanetary dust cloud with the orbits of the dust particles detected by the micrometeoroid experiment. Further analysis will be a consideration of the actual data, taking into account the described weighting in order to produce a picture of the orbital elements in the dust cloud similar to studies of meteors done before (Southworth and Sekanina, 1973).

References

Dietzel, H., Eichhorn, G., Fechtig, H., Grün, E., Hoffmann, H.-J., Kissel, J.: The HEOS 2 and HELIOS micrometeoroid experiments. J. Phys. E.: Sc. Instr. **6**, 209–217, 1973

Grün, E., Fechtig, H., Kissel, J., Gammelin, P.: Micrometeoroid data from the first two orbits of Helios 1. J. Geophys., **42**, 717–726, 1977

Grün, E., Kissel, J., Fechtig, H., Gammelin, P., Hoffmann, H.J.: Preliminary results of the micrometeoroid experiment on board Helios A. In: Interplanetary dust and zodiacal light, H. Elsässer, H. Fechtig, eds., Lecture Notes Phys. **48**, pp. 159–163. Berlin-Heidelberg-New York: Springer 1976

Schwehm, G.: Radiation pressure on interplanetary dust particle. In: Interplanetary dust and zodiacal light, H. Elsässer, H. Fechtig, eds., Lecture Notes Phys. **48**, pp. 459–463. Berlin-Heidelberg-New York: Springer 1976

Southworth, R.B., Sekanina, Z.: Physical and dynamical studies of meterors. NASA Contractor Report CR-2316, 1973

Received February 3, 1977; Revised Version May 9, 1977